applied optics

Calibration algorithm for cooled mid-infrared systems considering the influences of ambient temperature and integration time

SONGTAO CHANG* AND ZHOU LI

Changchun Institute of Optics, Fine Mechanics and Physics, Chinese Academy of Sciences, Changchun 130033, China
*Corresponding author: stchang2010@sina.com

Received 3 July 2019; revised 6 September 2019; accepted 10 September 2019; posted 11 September 2019 (Doc. ID 371648); published 10 October 2019

Midwave infrared systems with cooled detectors are generally used for high-precision or quantitative measurement, such as radiometry and thermometry. As a basis of these applications, radiometric calibration aims to obtain the relationship between the infrared images and the incident radiant flux generated by the scene or targets. Conventional radiometric calibration algorithms do not take the influences of integration and ambient temperature into consideration. As a consequence, the accuracy of calibration deteriorates whenever the temperature or the integration time varies. To solve this problem, we analyzed the effects of integration time and ambient temperature on coefficients of the radiometric calibration formula by theoretical and experimental analysis. Then, a radiometric calibration method is deduced to remove the variation of integration time and ambient temperature on the accuracy of calibration and radiometry. Several radiometric calibration experiments were conducted using a midwave infrared camera inside a chamber with controllable temperature. The results indicate that the proposed calibration algorithm is more effective and accurate, compared with conventional calibration methods, in complicated working conditions with variable integration times and ambient temperatures.

https://doi.org/10.1364/AO.58.008118

1. INTRODUCTION

Cooled infrared focal plane arrays, or IRFPAs, are the key components of high-end infrared imaging systems, which are used for radiometry and thermometry. For these quantitative measurement applications, accurate radiometric calibrations are essential. Radiometric calibration aims to obtain the relationship between the incident radiation and the output gray level in the infrared images. Conventional radiometric calibration methods are conducted at preselected integration times by using a blackbody. Their disadvantage is that once the ambient temperature or the integration time changes, the accuracy of the calibration decreases or even the calibration result defects. As a part of a thermal detection system, the infrared detector is sensitive to heat. Given that temperature of the detector or the optomechanical system changes with ambient temperature, the output gray level of the detector will change or drift if the ambient temperature changes [1–4]. Since the temperature of a cooled infrared detector is fairly stable, the drift caused by variation of the ambient temperature is mostly generated by radiance of the optomechanical system rather than the detector itself [5,6]. In conclusion, the radiometric calibration result is defect whenever the ambient temperature changes. Additionally, the integration time, or the exposure time, is another important influencing factor for radiometric calibration. It is definite that the output of a detector is linear to the integration time. Naturally, the relationship obtained by calibration will change whenever the integration time, or the exposure time, of a detector changes. It is concluded that calibration of the infrared system will be repeated to updating parameters of the calibration formula, if the ambient temperature or the integration time changes. In the other word, the calibration formula is dependent to the ambient temperature and the integration time. So, it is worthy to research the influence of integration time and ambient temperature on radiometric calibration.

This problem has been discussed in many literatures, which can be generally classified into three categories. (1) Some researchers pay attention to the influence of environmental temperature variation on the output gray levels of uncooled infrared detectors and have proposed several drift compensation methods based on the rule summarized from experimental tests [7–10]. These researches pay attention to uncooled infrared detectors, whose noise, stability, and uniformity are far worse than the cooled ones. Hence, they cannot fulfill the requirements of quantitative measurement, and the drift compensation methods are not applicable for cooled infrared systems. Besides, theoretical analysis of the influence of ambient temperature on radiometric calibration is not analyzed in these literatures. (2) On the basis of the linear relationship between the integration time and the output gray level of the infrared detector, M. Ochs proposed a pixel-wise calibration method. Upon this method, high dynamic range of the imaging system can be achieved by using fewer reference sources than traditional calibration methods [2,11]. This method yields the advantage of high-accuracy radiometric calibration, whereas it does not involve the influence of ambient temperature variation. (3) For cooled infrared systems, which are characterized by having cooled IRFPAs, the influences of ambient temperature on radiometric calibration mainly result from stray radiation. Stray radiation is generated by the lens, the lens baffle, and other mechanical structures whose temperatures exceed 0 K. It can be analyzed or calculated by using commercial programs such as Zemax and Tracepro [5,6,12,13]. However, the simulation results are not always credible as we expected. The reason lies in the significant error caused by ideal treatments of materials, bidirectional reflectance distribution function (BRDF), and characteristics of lens. In summary, the accuracy of the conventional radiometric calibration algorithm is greatly affected by the ambient temperature and the integration time. Furthermore, the influences of these two factors on radiometric calibration are not fully studied at present.

In this article, the effects of two factors, i.e., the ambient temperature and the integration time, are studied in detail by principle analysis. Based on this, we deduced a comprehensive calibration formula with four constant coefficients and three variables, namely the incident flux, the ambient temperature, and the integration time. It should be pointed out that traditional radiometric calibration formulas have only one variable, namely the incident flux. Finally, a calibration algorithm, which is effective in complex environmental conditions, is proposed in this paper based on the deduced calibration formula. In Section 2, the principle of the conventional radiometric calibration algorithm is introduced. Afterwards, we explain why the ambient temperature and the integration time influence the calibration formula. In Section 3, the principle of the influence of ambient temperature and integration time on the calibration formula is put forward. Then, a quantitative analysis method for the influences is proposed. Based on this, we deduced a comprehensive calibration formula and propose a novel calibration algorithm, which is effective in complex environmental conditions. Then, in Section 4, calibration experiments are carried out to verify the theories described above. It is concluded in Section 5 that the analysis of the influences are reasonable. Moreover, the proposed calibration formula and algorithm yield high accuracy under different ambient temperatures and integration times. In a word, the proposed algorithm considering the influence of ambient temperature and integration time is effective and accurate in complicated working conditions with variable integration times and ambient temperatures. It is, therefore, meaningful for practical applications of cooled infrared systems.

2. TRADITIONAL CALIBRATION ALGORITHM AND ITS DRAWBACKS

A. Principle of the Traditional Calibration Algorithm

There are two types of radiometric calibration methods: absolute calibration and relative calibration. The former, namely absolute calibration, is generally called calibration for short. It aims to obtain the absolute relationship between the incident energy and the output gray level of the detector. Hence, it is mainly used for radiometry or thermometry. The latter, i.e., relative calibration, refers to nonuniformity correction, or NUC. NUC is generally conducted to correct the photon response nonuniformity (PRNU) or fixed pattern noise (FPN) of detectors. The radiometric calibration algorithms herein belong to absolute calibration.

Radiometric calibration of an infrared imaging system is essential for radiometry and thermometry applications. Infrared systems used in these quantitative measurement applications are constrained to operate in a range of irradiance, within which the infrared detectors exhibit linear response. Among numerous calibration methods, The near-extended-source method is the most commonly used one [14–18]. As is shown in Fig. 1, an extended area blackbody is placed in front of the input pupil, or the entrance pupil, of an infrared system to illuminate the detectors, or IRFPAs, uniformly. The blackbody, whose emissivity is close to 1, is the most popular reference source for radiometric calibration. The temperature of the blackbody's emit area is controllable by heating or cooling, and its temperature accuracy is quite high compared with other infrared emitters.

The radiance $L(T_t)$ represents the radiation capacity of an emitter. It can be computed by using Plank's formula,

$$L(T_t) = \varepsilon \cdot \int_{\lambda_1}^{\lambda_2} L_\lambda(\lambda,\ T_t)\mathrm{d}\lambda$$

$$= \varepsilon \cdot \int_{\lambda_1}^{\lambda_2} \frac{C_1}{\lambda^4[\exp(C_2/\lambda T_t) - 1]}\mathrm{d}\lambda, \tag{1}$$

where ε is the emissivity of the blackbody source. $L_\lambda(\lambda,\ T_t)$, in units of $\mathrm{W \cdot m^{-2} \cdot sr^{-1}}$, denotes the spectral radiance of an ideal blackbody at temperature T_t in units of Kelvin. $\lambda_1 \sim \lambda_2$ is the wavelength range in units of μm. C_1, in units of $\mathrm{W \cdot \mu m^4 \cdot m^{-2}}$, is the first radiation constant. C_2, in units of $\mathrm{\mu m \cdot K}$, is the second radiation constant.

The output gray level [digital number (DN)] of a detector is given by the approximate linear relation,

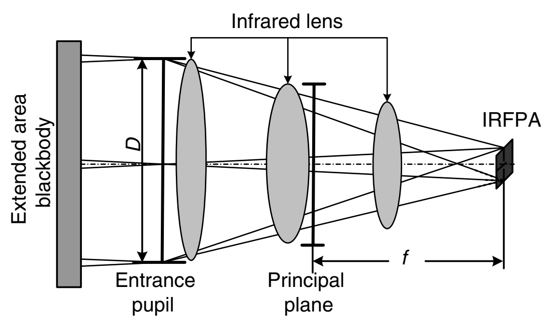

Fig. 1. Schematic diagram of near-extended-source method.

$$h_{i,j}(T_t) = G_{i,j} \cdot L(T_t) + O_{i,j}, \tag{2}$$

where $h_{i,j}$ is the gray value of the (i, j)th detector in the array, $G_{i,j}$ denotes the response associated with the radiance of the reference source, and $O_{i,j}$ is the offset. For simplicity, the subscript (i, j) is omitted in the subsequent formulas.

It is worth noting that when the camera is positioned very close to a blackbody for near-extended-source-based calibration, a narcissus (ghost image) may change the output gray level with an arbitrary pattern. This phenomenon is naturally harmful for the accuracy of radiometric calibration. In order to reduce the influence of this factor, one-point or two-point NUC is performed before radiometric calibration. Same as the visible light detector, the infrared detector output gray level h is linear to the integration time. G is obviously proportional to the integration time. It is worth noting that the internal structures, such as the lens and barrel, are radiation sources that will introduce stray radiation and contribute to O. In principle, this part of energy is proportional to the integration time. In addition, the stray radiation varies with the temperature of surrounding structures. So, the radiometric calibration formula is also related to the ambient temperature. It is recommended to update radiometric calibration when the integration time or the ambient temperature changes.

B. Evaluation of Radiometric Calibration Accuracy

High-precision radiometric calibration is essential for infrared radiometry or thermometry. So, the evaluation of radiometric calibration accuracy is naturally related to the principle of radiometry. Radiometry and thermometry are the reverse processes of radiometric calibration. The radiance or intensity of the measured target is obtained by substituting the gray level of the detector output into the calibration formula, namely Eq. (2). Specifically, the radiometric calibration accuracy can be evaluated by radiometry of a standard source, i.e., a blackbody is recommended. The radiance of the source can be measured and computed by using the output gray level and the calibration formula. The difference between the calculated radiance and the actual value, computed by Eq. (2), is defined as the radiometric calibration error, which represents the accuracy of radiometric calibration. The near-extended-source method shown in Fig. 1 is applicable to evaluate the accuracy of calibration. Setting the temperature of the source to T_0, we can get the output gray level h'. Then, the radiance $L'(T_0)$ can be computed by using Eq. (2). Inverting Eq. (2) results in

$$L'(T_0) = \frac{h' - O}{G}. \tag{3}$$

Hence, the radiometry error of the standard source, or the radiometric calibration error, can be computed by

$$E_c = \frac{L'(T_0) - L(T_0)}{L(T_0)} \times 100\%. \tag{4}$$

According to the experience of engineering applications, the radiometric calibration error that is acceptable is generally lower than 10%. For higher precision applications, lower than 5% may be required. The calibration error is mainly determined by the accuracy of the reference, the calibration method, the ambient temperature, and performance of the detector. For cooled infrared systems, radiometric calibration should be conducted in a short time to reduce the impact of ambient temperature instability.

3. PROPOSED RADIOMETRIC CALIBRATION ALGORITHM

A. Research on Effects of the Integration Time and the Ambient Temperature

To analyze the influence of the integration time and the ambient temperature on radiometric calibration, we first focus on the calibration formula, namely Eq. (2). G is the response rate of the infrared system to the blackbody radiance. It is generally determined by the detector response and parameters of the optical system. We assume that the response of an infrared detector to the received 1 J radiant energy is R, and the integration time or the exposure time is named t. The radiation flux received by a detector element is denoted by Φ_t. Therefore, Eq. (2) is equivalent to

$$h(T_t) = R \cdot \Phi_t \cdot t + O. \tag{5}$$

Given parameters of the infrared optical system in Fig. 1, the incident flux that reaches a single detector of the IRFPAs can be expressed by

$$\Phi_t = \frac{\pi \cdot \tau_{\text{opt}}}{4} \cdot \left(\frac{D}{f}\right)^2 \cdot A_d \cdot L(T_t) \cdot \cos^4\theta, \tag{6}$$

where τ_{opt} denotes the transmittance of the infrared lens, D denotes the diameter of the input pupil, f is the focal length, and A_d is the sensitive area of a detector in the IRFPA. θ is the angle between the chief ray of a single detector (or pixel) and the optical axis. For a small field-of-view (FOV) imaging system when focusing at infinity, $\cos^4\theta$ is approximately equal to 1. The response G is therefore given by

$$G = \frac{\pi \cdot \tau_{\text{opt}}}{4} \cdot \left(\frac{D}{f}\right)^2 \cdot A_d \cdot R \cdot t, \tag{7}$$

where τ_{opt} is the transmittance of the optical system, which varies extremely slow versus ambient temperature. D and f are optical parameters that are generally considered to be independent to ambient temperature. The detector area A_d is naturally unrelated to the ambient temperature. Cooled infrared detectors are known to work at a stabilized temperature, so the response of a detector would hardly vary with the ambient temperature. R is determined by the detector's quantum efficiency and overall system gain in units DN/e-, which is defined as a key parameter of a imager in EMVA Standard 1288. Cooled infrared detectors are known to work at a stabilized temperature. So, fluctuations of the quantum efficiency and the overall system gain are ignored generally. In other words, the responses of cooled detectors are independent to the ambient temperature. The response G is therefore proportional to the integration time t for an infrared imaging system.

The offset O in Eq. (5) is the gray level of a detector that was caused by stray radiation of the infrared imaging system, ambient radiation reflected by the lens, and internal factors of the detector.

Stray radiation, which is defined as the infrared radiation out of the FOV of the optical system, mainly results from radiation of the lens, radiation emitted or reflected by the housing cone, and other mechanical structures. They finally reach the infrared detector element through numerous optical paths. The paths are composed by transmitting, reflecting, absorbing, and scattering [5]. Due to heat conduction, the temperature of optical components tends be close to the ambient temperature. The radiation of the lens and other components can be calculated by using their temperature and surface emission. As illustrated in Eq. (1), the radiance of an object at temperature T_t is the product of surface emission ε and $L(T_t)$, which denotes the radiance of an ideal blackbody at the same temperature. As a consequence, the contribution of stray radiation on radiometric calibration is almost proportional to the radiance of an ideal blackbody at ambient temperature, as well as the integration time [10].

The reflected ambient radiation flux that reaches the infrared detector can be expressed by

$$\Phi_b = \frac{\pi(1-\varepsilon)\tau_{\text{opt}}}{4}\left(\frac{D}{f}\right)^2 \cdot A_d \cdot L(T_a) = k_b \cdot L(T_a), \tag{8}$$

where T_a is the ambient temperature. $L(T_a)$ can be calculated by Eq. (2). Given an infrared system, k_b is determined by the emission of the reflecting surface, the transmittance of the lens, the pupil diameter, and the focal length. These four parameters change quite slowly with time; hence, they are considered as a constant for most applications. Equation (8) indicates that the flux Φ_b is also directly proportional to $L(T_a)$. Hence, the gray level generated by reflected ambient radiation is proportional to the integration time and the radiance $L(T_a)$. So, the gray level introduced by stray radiation and reflected ambient radiation can be written as a function of $L(T_a)$,

$$h_s = t \cdot G_s \cdot L(T_a). \tag{9}$$

Internal factors of the detector contribute to the dark signal, which is described by the output gray level of a detector with zero irradiation. The dark signal, as a portion of offset, mainly contains radiation generated by the dewar for cooling, the dark current, and the dark level. Note that the temperature in dewar is stable for a cooled infrared system. The stray radiations generated by dewar and its cold shield are therefore ambient temperature dependent but proportional to the integration time. The dark current generally depends on the temperature and the integration time of an infrared detector. Given that the temperature of a cooled detector is constant, the dark current is also proportional to the integration time. These two portions of offset can be expressed by $t \cdot h_{dc}$. The dark level as defined in EMVA Standard 1288 is ambient temperature and integration independent. It is denoted by h_{dl} in this paper.

B. Proposed Radiometric Calibration Algorithm

Based on the analysis above, we propose a radiometric calibration formula that considers parameters, namely the integration time and the ambient temperature. The calibration model or formula can be written as

$$h(t, T_a, T_t) = t \cdot G_n \cdot L(T_t) + t \cdot G_s \cdot L(T_a) + t \cdot h_{dc} + h_{dl}. \tag{10}$$

t is the integration time in units of second. G_n, therefore, is redefined as the normalized response in units of $\mathrm{DN} \cdot \mathrm{m}^2 \cdot \mathrm{sr} \cdot \mathrm{W}^{-1} \cdot \mathrm{s}^{-1}$. $t \cdot G_s \cdot L(T_a)$ denotes the gray level generated by the stray radiation and the reflected ambient radiation. $t \cdot h_{dc} + h_{dl}$ represents the effects of internal factors of the detector.

Fundamental of the proposed calibration is to calculate the four parameters (G_n, G_s, h_{dc}, and h_{dl}) in Eq. (10). For ease of description, the calibration formula can be written as

$$f(x, y, z) = G_n \cdot xy + G_s \cdot xz + h_{dc} \cdot x + h_{dl}, \tag{11}$$

where

$$\begin{cases} x = t \\ y = L(T_t) \\ z = L(T_a) \\ f(x, y, z) = h(t, T_a, T_t) \end{cases}. \tag{12}$$

The residual error can be defined by

$$\varepsilon_i = (G_n \cdot x'_i \cdot y'_i + G_s \cdot x'_i \cdot z'_i + h_{dc} \cdot x'_i + h_{dl}) - f'_i, \tag{13}$$

where f'_i denotes the gray level of a detector that is imaging the reference source at temperature $T'_{t\,i}$. The ambient temperature is $T'_{a\,i}$, and the integration time is x'_i.

According to the principle of the least squares method, G_n, G_s, h_{dc}, and h_{dl} can be calculated by solving

$$\begin{bmatrix} x'_1y'_1 & x'_1z'_1 & x'_1 & 1 \\ x'_2y'_2 & x'_2z'_2 & x'_2 & 1 \\ \vdots & \vdots & \vdots & \vdots \\ x'_ny'_n & x'_nz'_n & x'_n & 1 \end{bmatrix} \begin{bmatrix} G_n \\ G_s \\ h_{dc} \\ h_{dl} \end{bmatrix} = \begin{bmatrix} f'_1 \\ f'_2 \\ \vdots \\ f'_n \end{bmatrix}. \tag{14}$$

The calibration parameters above can be obtained from at least four images captured at different integration times, blackbody temperatures, and ambient temperatures. It is important to note that the gray levels f'_i shall not be saturated, in order to maintain the linear response model that is supposed. The parameters are substituted into Eq. (10) to obtain the calibration formula. Afterwards, we can use the equation to speculate the calibration formulas at various ambient temperatures and integration times. Then, the accuracy of the proposed calibration formulas can be evaluated by radiometric calibrations conducted under other integration times, blackbody temperatures, and ambient temperatures. According to engineering experiences, radiometric calibration accuracy within 5% is acceptable for general applications.

4. EXPERIMENTS

Several radiometric calibration experiments were conducted to verify the analysis and the proposed calibration algorithm. A midwave infrared camera with a 640 × 512 resolution cooled IRFPA and an infrared imaging lens with a 50 mm focal length were used to form an infrared imaging system for radiometric

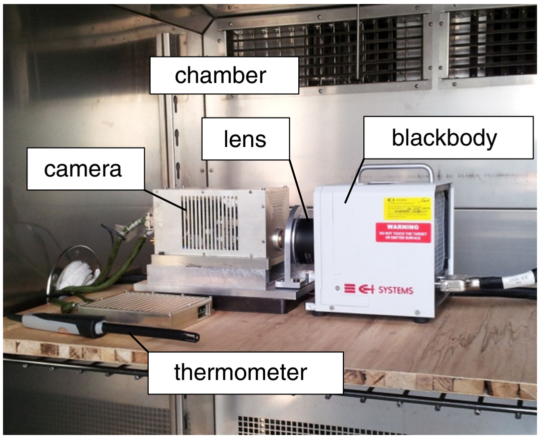

Fig. 2. Experimental setup for radiometric calibration.

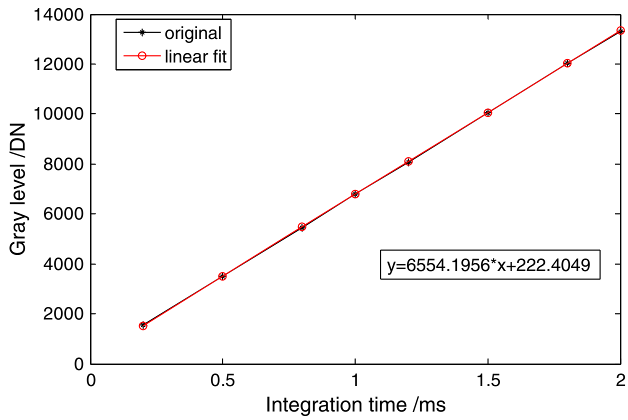

Fig. 3. Gray level as a function of the integration time.

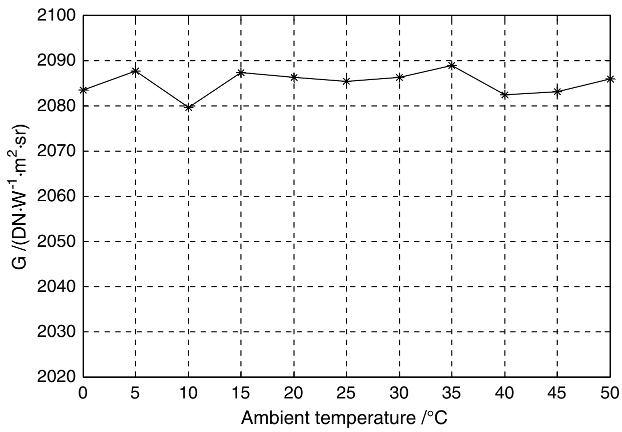

Fig. 4. Gains versus the ambient temperatures.

calibration. The camera was HRC Minicore 300Z, manufactured by FLIR Systems in USA. The NETD@22°C of this cooled camera is lower than 20 mK in typical. The IRFPAs, with 14-bit digital output, are sensitive in the 3.7–4.8 μm wave band for imaging. Besides, the pixel size of the IRFPAs is 15 μm. The FOV of this infrared imaging lens is about 3° × 3°, which is quite narrow. The reference for near-extended-source calibration is an extended blackbody, namely SR800-R, which is produced by CI-Systems, a worldwide supplier of electro-optical test and measurement equipment in Israel. Its emissivity reaches 0.97 in the 3.7–4.8 μm wave band. The emit surface of radiation is about 100 × 100 mm, with controllable temperature in range of 0–125°C, and the accuracy is about 0.01°C.

Figure 2 illustrates the setup of these calibration experiments. The blackbody, the lens, the camera, and a thermometer were put into a chamber whose inside temperature can be set in the range of 0°C–50°C. The inside temperature, therefore, can be regarded as the ambient temperature of the infrared imaging system for radiometric calibration experiments. To measure the internal temperature more accurately, a thermometer with ±0.1°C accuracy was put in the chamber. According to the performance list of this chamber, the accuracy of ambient temperature reaches ±0.2°C, which fulfills the requirements of our experiments. Besides, the inside temperature can be stabilized in about 5 min once it is set to a higher or lower one.

A. Output Gray Level as a Function of Integration Time

By setting the blackbody to 50°C and changing the integration time from 0.2 ms to 2 ms, we obtained the relation between the integration times and the gray levels, as shown in Fig. 3. It can be concluded that the gray level is almost a perfect linear function of the integration time.

B. Gain as a Function of Ambient Temperature

To verify the conclusion that the gain G_n is independent to the ambient temperature, calibrations at different ambient temperatures are conducted. Figure 4 illustrates that the differences of the gains are less than 0.45% when the ambient temperature ranges from 0°C to 50°C. The variation is obviously negligible for most applications of radiometric calibration. In summary, the gain G_n is independent to the ambient temperature.

C. Obtain the Calibration Formula Using the Proposed Algorithm

To evaluate the proposed calibration correction method, several near-extended-source radiometric calibration experiments were performed in a chamber with controllable temperatures inside. First of all, we conducted an experiment to obtain the calibration formula, i.e., Eq. (10), and the steps are as follows:

(1) Set the inside temperature, i.e., the ambient temperature, to 20°C to capture images of the blackbody at temperatures, namely 40°C and 50°C. The integration times of this infrared camera are set to 0.5 ms and 1 ms.
(2) The inside temperature is then set to 30°C to calibrate the infrared imaging system in the same way as step (1).
(3) Output gray levels of a detector, or a pixel, in all the images that captured are picked out and listed in Table 1.

The pixel with location (320,256), in units of pixel, is used to evaluate the proposed calibration method. For the lens with a narrow FOV, for example 3°, $\cos^4\theta$ is approximately equal to

Table 1. Data for Acquiring the Calibration Formula

Integration Time/ms	Ambient Temperature/°C	Blackbody Temperature/°C	Output Gray Level of a Detector/DN
0.5	20	40	2339
1	20	40	4608
0.5	30	40	2397
1	30	40	4726
0.5	20	50	3150
1	20	50	6208
0.5	30	50	3201
1	30	50	6318

1. So, the proposed calibration method is effective for each pixel in applications that do not require extremely high calibration accuracy.

By substituting the data into Eq. (12), we computed the parameters, namely x_i', y_i', z_i', and f_i'. They were afterwards substituted into Eq. (14) to obtain an overdetermined linear equation.

Calibration parameters, namely G_n, G_s, h_{dc}, and h_{dl}, can be obtained by solving the above equation with the least squares method. Then, the radiometric calibration formula was obtained,

$$h(t, T_a, T_t) = 2.0761 \times 10^6 t L(T_t) + 2.5879 \times 10^5 t L(T_a) + 1.3324 \times 10^5 t + 78.50. \tag{15}$$

It is important to note that the integration time here is in units of seconds.

D. Influence of the Ambient Temperature and the Integration Time on Calibration Error

For the purpose of evaluating the calibration accuracy of the proposed method, we acquired more images of a blackbody under various ambient temperatures and integration times. The experiments were performed at the ambient temperature varying from 0°C to 50°C, 5°C as the interval, while the integration time varies from 0.2 ms to 2 ms. As is known, the proposed calibration method aims to remove the restriction of the ambient temperature and the integration time on radiometric calibration. The blackbody, however, yields high temperature accuracy, i.e., 0.01°C. We selected several blackbody temperatures ranging from 30°C to 60°C for imaging.

We chose the data, or the calibration images, at one exposure time and a single blackbody temperature to analyze the influence of change in ambient temperature on the accuracy of radiometric calibration. Subsequently, we evaluated the compensation ability of the proposed calibration algorithm on accuracy loss caused by variation of ambient temperature. The images of a blackbody at 30°C, captured at integration time 0.001 s (or 1 ms) are selected at ambient temperatures ranging from 0°C to 50°C.

Using the conventional radiometric calibration method, the calibration was performed at ambient temperature 20°C. We get the radiometric calibration formula

$$h = 2076.38 \times L(T_t) + 462.67. \tag{16}$$

Using the proposed calibration algorithm, the calibration formula was established by Eq. (15),

$$h(t, T_a, T_t) = 2076.10 \times L(T_t) + 258.79 \times L(T_a) + 211.74. \tag{17}$$

The blackbody radiance $L(T_t)$ at 30°C is $1.4106\ \mathrm{W \cdot m^{-2} \cdot sr^{-1}}$, and as a reference value, the radiometric calibration errors of the two methods are evaluated. $L(T_a)$ is calculated by Eq. (1) at different ambient temperatures, and the results are shown in Fig. 5.

The effect of ambient temperature on the accuracy of different calibration methods is illustrated in Fig. 6.

For the conventional calibration algorithm, the calibration formula is obtained at ambient temperature 20°C. Figure 6 shows that the accuracies of these two calibration algorithms are equivalent, lower than 1%. When the ambient temperature is far from the calibration temperature 20°C, accuracy of the conventional radiometric calibration method deteriorates. As the ambient temperature further increases or decreases, the radiometric calibration error can reach 15%, which is unacceptable in almost all cases.

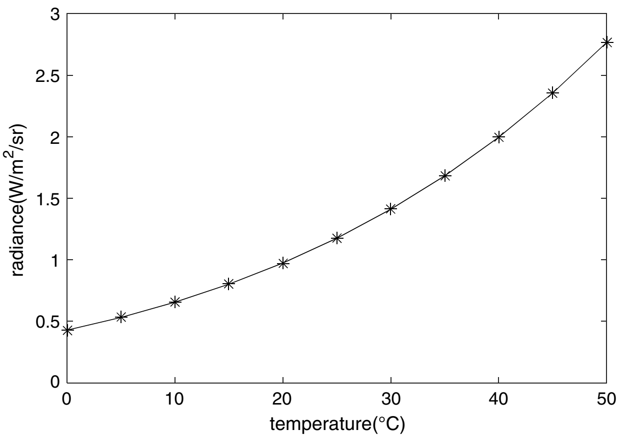

Fig. 5. Radiance as a function of temperature.

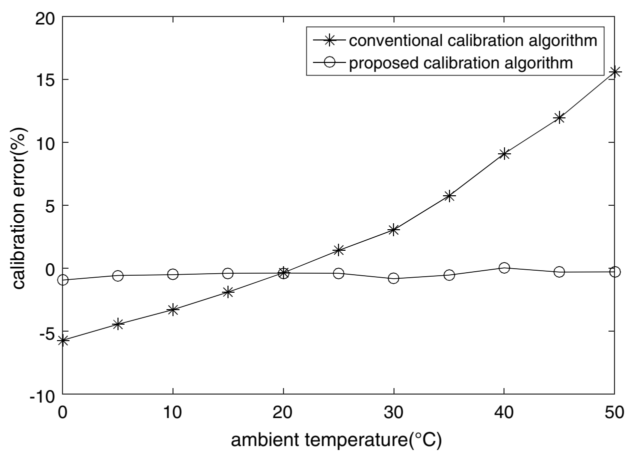

Fig. 6. Effect of the ambient temperature on calibration accuracy.

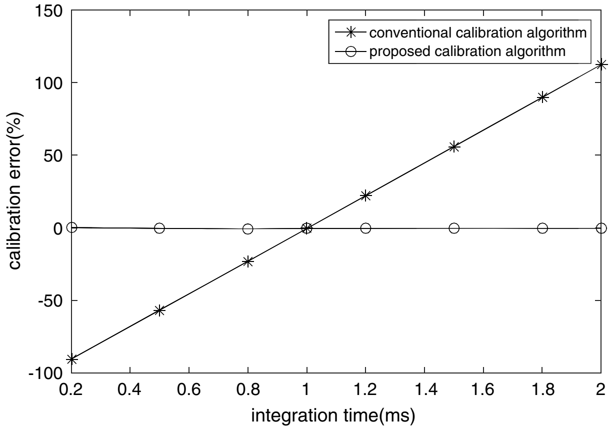

Fig. 7. Effect of the integration time on calibration accuracy.

On the contrary, the proposed calibration algorithm performs well at multiple ambient temperatures. The calibration errors at these ambient temperatures are decreased to less than 1% by using the proposed calibration algorithm, which means that the method can effectively compensate the calibration error caused by environmental temperature changes. It is indicated that the proposed algorithm in this paper can be used to compensate the calibration formula according to the ambient temperature.

In addition, the response of an infrared detector is linear to the integration time, so a single calibration formula cannot be used for different exposure times. Figure 7 shows that the calibration at 1 ms causes excessive calibration errors when it is used for other integration times. These errors are obviously unacceptable. As a result, it is not allowed to use a single calibration formula for an infrared system working at multiple integration times. However, by using the proposed calibration algorithm in this paper, the calibration error for each exposure time is less than 1%, which is satisfactory.

E. Analyze the Calibration Error of the Proposed Algorithm Statistically

In order to analyze the calibration accuracy of the proposed algorithm comprehensively, we processed more experimental data under multiple ambient temperatures and integration time for statistical analysis.

For the benefit of expression, we call a combination of an ambient temperature, an integration time, and a blackbody temperature as a working condition of an infrared imager. The conditions that have not been used to obtain the calibration formula, namely Eq. (15), are selected to evaluate the performance of the proposed calibration method. There are altogether 352 conditions. Eight of them were used for calibration, and 14 out of the other 344 conditions were excluded because of image saturation. Therefore, 330 conditions, or images, were used for estimating the calibration error. Section 2.B illustrates the calculation algorithm of the calibration error. Calibration errors of these conditions are shown in Fig. 8.

Figure 8 illustrates that the maximum calibration error of the proposed method is −1.36% and the standard deviation is 0.39%, which is far less than 5%. In summary, the calibration accuracy of the proposed method is reliable at ambient temperatures ranging from 0 to 50°C and arbitrary integration times between 0.2 ms and 2 ms.

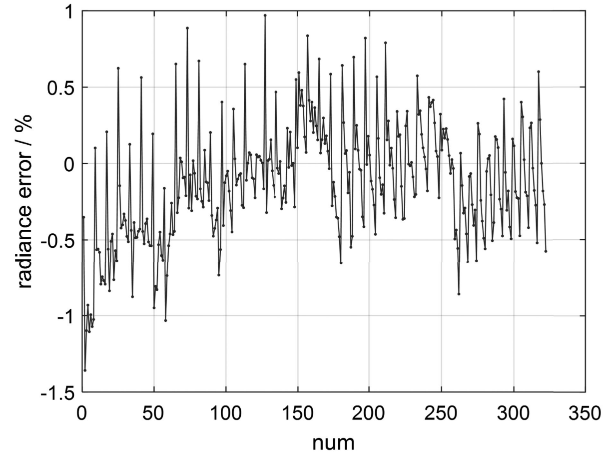

Fig. 8. Calibration errors of 330 conditions.

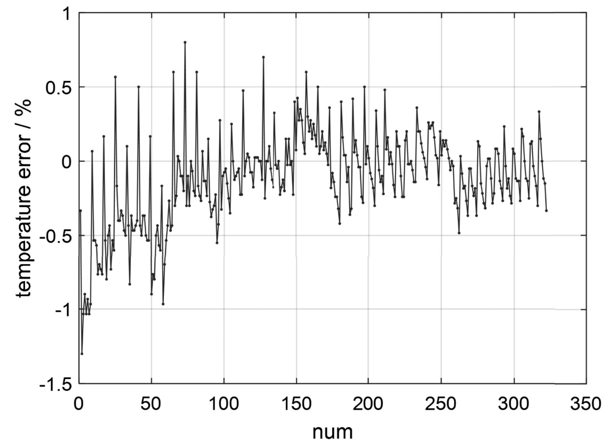

Fig. 9. Temperature errors caused by the proposed calibration method.

The infrared imaging systems used in scientific applications pay more attention to the measurement of radiance. However, the absolute and relative accuracy of temperature measurement may be concerned in other scenarios. Figure 9 shows the thermometry errors generated by the radiometric calibration errors that result from the proposed calibration method.

As is shown in Fig. 9, the maximum relative temperature error of the proposed method is −1.30%, and the standard deviation is 0.31%. Additional data show that the maximum absolute temperature error is −0.39°C and the standard deviation is 0.11°C. It is illustrated by the data above that the proposed calibration algorithm in this paper yields little influence on the accuracy of thermometry.

The experimental results show that the proposed calibration method yields high radiometric calibration accuracy, and can be applied at ambient temperatures in the range of 0°C–50°C. That is to say, as long as the radiometric calibration is performed under two ambient temperatures and two integration times, a high-precision calibration formula for all integration times and ambient temperatures can be obtained by using the proposed method. This method improves the adaptability of the infrared system to various ambient temperatures. In addition, the integration time of the infrared camera can be set according to the scene radiance whenever necessary, instead of having only a few presupposed integration times that are available. Meanwhile, the radiometry or temperature accuracy would not be decreased by using the uncalibrated integration times. In conclusion, the radiometric calibration algorithm proposed herein yields high accuracy of calibration at arbitrary ambient temperatures and integration times.

5. CONCLUSION

This paper proposes a radiometric calibration method considering two additional parameters, namely the ambient temperature and the integration time, for cooled infrared systems. The most important two tasks of the article are the following: (1) analyze effects of the ambient temperature as well as the integration time on the output gray level; (2) deduce a calibration formula related to the two parameters. Based on these achievements, we deduce linear equations with blackbody images captured at two ambient temperatures and two integration times. Solving Eq. (14) by the least squares method, the calibration formula can be computed. Finally, several radiometric calibration experiments are performed in a chamber with controllable temperature to evaluate performance of the proposed calibration algorithm. Experimental results illustrate that the proposed calibration algorithm yields high calibration accuracy at arbitrary ambient temperature and integration time. It improves the adaptability of the system to the ambient temperature, as well as gives the user the freedom to optimize the detector output to the current scenery by changing the integration time. It is important to note that the proposed calibration method is effective for cooled infrared systems rather uncooled ones.

REFERENCES

1. I. Klapp, S. Papini, and N. Sochen, “Radiometric imaging by double exposure and gain calibration,” Appl. Opt. **56**, 5639–5647 (2017).
2. M. Ochs, A. Schulz, and H.-J. Bauer, “High dynamic range infrared thermography by pixelwise radiometric self calibration,” Infrared Phys. Technol. **53**, 112–119 (2010).
3. T. Svensson and I. Renhorn, “Evaluation of a method to radiometric calibrate hot target image data by using simple reference sources close to ambient temperature,” Proc. SPIE **7662**, 76620X (2010).
4. P. W. Nugent, J. A. Shaw, and N. J. Pust, “Correcting for focal-plane-array temperature dependence in microbolometer infrared cameras lacking thermal stabilization,” Opt. Eng. **52**, 061304 (2013).
5. E. Fest, *Stray Light Analysis and Control* (SPIE, 2013).
6. A. V. Pravdivtsev and M. N. Akram, “Simulation and assessment of stray light effects in infrared cameras using non-sequential ray tracing,” Infrared Phys. Technol. **60**, 306–311 (2013).
7. S. D. Dong, X. F. Yang, and B. He, “A transplantable compensation scheme for the effect of the radiance from the interior of a camera on the accuracy of temperature measurement,” Int. J. Infrared Millimeter Waves **27**, 1517–1528 (2006).
8. S. D. Dong, X. F. Yang, and W. Yang, “A method for removing effect of the camera radiance on infrared image,” Int. J. Infrared Millimeter Waves **29**, 499–507 (2008).
9. X. B. Sui, Q. Chen, and G. H. Gu, “Nonuniformity correction of infrared images based on infrared radiation and working time of thermal imager,” Optik **124**, 352–356 (2013).
10. S. T. Chang, Y. Y. Zhang, Z. Y. Sun, and M. Li, “Method to remove the effect of ambient temperature on radiometric calibration,” Appl. Opt. **53**, 6274–6279 (2014).
11. Y. Jin, J. Jiang, and G. G. Zhang, “Three-step nonuniformity correction for a highly dynamic intensified charge-coupled device star sensor,” Opt. Commun. **285**, 1753–1758 (2012).
12. Y. Liu, X. Q. An, and Q. Wang, “Accurate and fast stray radiation calculation based on improved backward ray tracing,” Appl. Opt. **52**, B1–B9 (2013).
13. S. M. Nejad, A. B. Madineh, and M. Nasiri, “Baffle design and evaluation of the effect of different parameters on its performance,” Optik **124**, 6480–6484 (2013).
14. M. D. Mermelstein, K. A. Snail, and R. G. Priest, “Spectral and radiometric calibration of midwave and longwave infrared cameras,” Opt. Eng. **39**, 347–352 (2000).
15. W. L. Wolfe, *Introduction to Radiometry* (SPIE, 1998).
16. B. G. Grant, *The Art of Radiometry* (SPIE, 2009).
17. G. C. Holst, *Testing and Evaluation of Infrared Imaging Systems* (JCD, 1933).
18. S. Papini, P. Yafin, I. Klapp, and N. Sochen, “Joint estimation of unknown radiometric data, gain, and offset from thermal images,” Appl. Opt. **57**, 10390–10401 (2018).